Vol 10 No 6, June 2001
1009-1963/2001/10(06)/0541-09

Chinese Physics

© 2001 Chin. Phys. Soc.
and IOP Publishing Ltd

GINZBURG-LANDAU THEORY AND VORTEX LATTICE OF HIGH-TEMPERATURE SUPERCONDUCTORS*

ZHOU SHI-PING(周世平)

Department of Physics, Shanghai University, Shanghai 200436, *China*

(Received 24 September 2000; revised manuscript received 23 December 2000)

The thermodynamics of the vortex lattice of high-temperature superconductors has been studied by solving the generalized Ginzburg-Landau equations derived microscopically. Our numerical simulation indicates that the structure of the vortex lattice is oblique at the temperature far away from the transition temperature T_c, where the mixed s$-$d$_{x^2-y^2}$ state is expected to have the lowest energy. Whereas, very close to T_c, the d$_{x^2-y^2}$ wave is slightly lower energetically, and a triangular vortex lattice recovers. The coexistence and the coupling between the s and d waves would account for the unusual dynamic behaviours such as the upward curvature of the upper critical field curve $H_{C2}(T)$, as observed in dc magnetization measurements on single-crystal $YBa_2Cu_3O_7$ samples.

Keywords: Ginzburg-Landau theory, vortex lattice, high-temperature superconductor
PACC: 7460E, 7460J, 7420

I. INTRODUCTION

Although there has been no agreement on a complete theory of high-temperature superconductors, a consensus has formed that the strong electron repulsion and the interlayer coupling of the quasi-two-dimensional layered nature of these materials are responsible for their anomalous physical properties. The repulsive electron interaction in the materials tends to increase the spin moments because it reduces the probability of two electrons with opposite spins occupying the same orbital and hence breaks the cancellation of the spin moments. An antiferromagnetic (AF) exchange interaction occurs between these induced spin moments since an electron can hop to the neighbouring site without violating Pauli's exclusion principle if the spin there is antiparallel. Consequently, an AF magnetic long range ordering and the singlet pair d-wave state is expected to form.[1,2] More recently, a theory based on $SO(5)$ symmetry proposed by Zhang favours also the d$_{x^2-y^2}$ pairing symmetry in the high-T_c superconductors.[3] Experiments[4,5] that probe the pairing symmetry using corner SQUIDs and tricrystal junctions provide evidence supporting a d$_{x^2-y^2}$ wave state in high-T_c $YBa_2Cu_3O_7$ superconductor. This issue remains controversial, however, because the electron-phonon interaction enhanced by interlayer pair tunnelling discussed by Anderson and co-workers predicts an anisotropic s-wave symmetry.[6] Also, the work of Liechtenstein *et al.*[7] suggests that although the AF spin fluctuation mechanism leads to the d pairing for a single layer, it would lead to a two-dimensional s symmetry for a bilayer if a sufficient strong AF correlation exists between the two layers. Support for the presence of significant s-wave component in this material may be readily found in Refs.[8–10].

In order to identify the different competing ground states, an effective Hamiltonian is needed. Anderson[11] and Rice and Zhang[12] argued rather successfully that a good starting point for modelling the strong correlation in the oxides should be the Hubbard, or the t-J models close to half-filling. Unfortunately, the exact solutions to these models in one dimension shed very little light on how to solve them in higher dimension cases. Even within the simplified Hubbard, there are two different energy scales in the problem.[13] Fortunately, near the normal to superconductive phase transition temperature T_c, the classification of superconducting states can be formulated entirely in terms of macroscopic Ginzburg-Landau (G-L) theory and requires no knowledge of the microscopic details of the superconductivity. Furthermore, away from T_c, for the layered structure with either the orthorhombic or the tetragonal lattices, the classification scheme remains unchanged.[14] Therefore, an appropriate G-L model may be an alternative starting point to study high-T_c superconductivity. In this paper, we will derive the G-L equations form the Gor'kov model by using the finite temperature Green's func-

*Project supported by the Foundation for University Key Teachers by the Ministry of Education, China.

tion method. The vortex structure is studied from the established G-L equations. The most remarkable feature of the vortex structure is that a triangle vortex lattice to an oblique vortex lattice is numerically indicated because a substantial s-wave component with fourfold symmetry spatially is induced in the core of the $d_{x^2-y^2}$ wave superconductor as the temperature goes down from T_c. This vortex transition may account for the unusual transport behaviours, such as the resistance transition curve broadening under the external magnetic field and the upward curvature of the upper critical magnetic field $H_{c2}(T)$ near the critical temperature in high-T_c superconductors.

Ⅱ. THE GINZBURG-LANDAU MODEL

Starting with the Gor'kov equations,[15] we derive equations for the $\boldsymbol{k}$ dependence of the order parameter, from which the G-L equations is formulated, and the G-L free energy is parameterized microscopically.

$$\begin{aligned}
&\left\{\mathrm{i}\omega_n - \frac{1}{2m}(-\mathrm{i}\nabla + e\boldsymbol{A})^2 + \mu\right\} G(\boldsymbol{x},\boldsymbol{x}',\omega_n) \\
&+ \int \mathrm{d}\boldsymbol{x}''\Delta(\boldsymbol{x},\boldsymbol{x}'')F^+(\boldsymbol{x}'',\boldsymbol{x}',\omega_n) = \delta(\boldsymbol{x}-\boldsymbol{x}'), \\
&\left\{-\mathrm{i}\omega_n - \frac{1}{2m}(\mathrm{i}\nabla + e\boldsymbol{A})^2 + \mu\right\} F^+(\boldsymbol{x},\boldsymbol{x}',\omega_n) \\
&+ \int \mathrm{d}\boldsymbol{x}''\Delta(\boldsymbol{x},\boldsymbol{x}'')G^*(\boldsymbol{x}'',\boldsymbol{x}',\omega_n) = 0, \qquad (1)
\end{aligned}$$

where G and F are, respectively, the single particle and pair propagators, and $\omega_n = (2n+1)\pi T$. The order parameter $\Delta(\boldsymbol{x},\boldsymbol{x}')$ in real space is defined as

$$\Delta^*(\boldsymbol{x},\boldsymbol{x}') = V(\boldsymbol{x}-\boldsymbol{x}')T\sum_{\omega_n} F^+(\boldsymbol{x},\boldsymbol{x}',\omega_n), \qquad (2)$$

with $-V(\boldsymbol{x}-\boldsymbol{x}')$ being the effective pairing interaction between two carriers. Substituting Eq.(1) into Eq.(2), we find to the third order in Δ

$$\begin{aligned}
\Delta^*(\boldsymbol{x},\boldsymbol{x}') =& V(\boldsymbol{x}-\boldsymbol{y})T\sum_{\omega_n}\Big\{\int \mathrm{d}\boldsymbol{x}'\mathrm{d}\boldsymbol{x}'' \\
&\cdot G_0(\boldsymbol{x}',\boldsymbol{x},-\omega_n)\Delta^*(\boldsymbol{x},\boldsymbol{x}'')\Big[G_0(\boldsymbol{x}'',\boldsymbol{y},\omega_n) \\
&- \int \mathrm{d}\boldsymbol{x}_1\mathrm{d}\boldsymbol{x}_2 G_0(\boldsymbol{x}'',\boldsymbol{x}_1,\omega_n)\Delta(\boldsymbol{x}_1,\boldsymbol{x}_2) \\
&\cdot \int \mathrm{d}\boldsymbol{x}_3\mathrm{d}\boldsymbol{x}_4 G_0(\boldsymbol{x}_3,\boldsymbol{x}_2,-\omega_n) \\
&\cdot \Delta^*(\boldsymbol{x}_3,\boldsymbol{x}_4)G_0(\boldsymbol{x}_4,\boldsymbol{y},\omega_n)\Big]\Big\}, \qquad (3)
\end{aligned}$$

where G_0 is the Green's function of free electrons in magnetic field $\boldsymbol{B} = \nabla\times\boldsymbol{A}$. Since only the electrons that are near the Fermi surface will join in the pairing process, and in considering that the Fermi wavelength is much less than the London penetration depth, G_0 can be expressed in terms of the zero-field Green's function $\tilde{G}_0$ as follows:[14]

$$G_0(\boldsymbol{x},\boldsymbol{x}',\omega_n) \approx \tilde{G}_0(\boldsymbol{x},\boldsymbol{x}',\omega_n)\mathrm{e}^{-\mathrm{i}e\boldsymbol{A}(\boldsymbol{x})\cdot(\boldsymbol{x}-\boldsymbol{x}')}, \qquad (4)$$

with $\tilde{G}_0(\boldsymbol{x},\omega_n) = \dfrac{1}{(2\pi)^2}\displaystyle\int \mathrm{d}\boldsymbol{k}\mathrm{e}^{\mathrm{i}\boldsymbol{k}\cdot\boldsymbol{x}}\frac{1}{\mathrm{i}\omega_n - \varepsilon_k}$.

Here $\varepsilon_k = (\boldsymbol{k}^2/2m) - \mu$ is the kinetic energy of the charge particle with mass m measured from the chemical potential μ. We introduce the centre of mass coordinates $\boldsymbol{R} = (\boldsymbol{x}+\boldsymbol{y})/2, \boldsymbol{R}' = (\boldsymbol{x}'+\boldsymbol{x}'')/2$, and the relative coordinates $\boldsymbol{r} = \boldsymbol{x}-\boldsymbol{y}, \boldsymbol{r}' = \boldsymbol{x}'-\boldsymbol{x}''$.

Taking account of the fact that the vector potential $\boldsymbol{A}$ varies slowly over the scale of the coherence length ξ, we assume that the magnetic field acts only on the centre of the paired particle and $\boldsymbol{A}(\boldsymbol{x}) = \boldsymbol{A}(\boldsymbol{y}) = \boldsymbol{A}(\boldsymbol{R})$ holds approximately. Performing the Fourier transformation of Eq.(4) with respect to the relative coordinate, we arrive at

$$\Delta^*(\boldsymbol{R},\boldsymbol{k}) \equiv \Delta_1^*(\boldsymbol{R},\boldsymbol{k}) + \Delta_2^*(\boldsymbol{R},\boldsymbol{k}), \qquad (5a)$$

with

$$\begin{aligned}
\Delta_1^*(\boldsymbol{R},\boldsymbol{k}) =& \int \frac{\mathrm{d}\boldsymbol{k}'}{(2\pi)^2}V(\boldsymbol{k}'-\boldsymbol{k})\Big\{T\sum_{\omega_n}\frac{1}{\omega_n^2+\varepsilon_{k'}^2} \\
&+ \frac{T}{2}\sum_{\omega_n}\Big[\frac{1}{(2m)^2}\frac{2\varepsilon_{k'}^2 - 6\omega_n^2}{(\omega_n^2+\varepsilon_{k'}^2)^3}(k_x'^2\Pi_x^2 + k_y'^2\Pi_y^2) \\
&- \frac{1}{2m}\frac{\varepsilon_{k'}}{(\omega_n^2+\varepsilon_{k'}^2)^2}\Pi^2\Big]\Big\}\Delta^*(\boldsymbol{R},\boldsymbol{k}'), \qquad (5b)
\end{aligned}$$

and

$$\begin{aligned}
\Delta_2^*(\boldsymbol{R},\boldsymbol{k}) =& -\int \frac{\mathrm{d}\boldsymbol{k}}{(2\pi)^2}V(\boldsymbol{k}-\boldsymbol{k}')T \\
&\cdot\sum_{\omega_n}\frac{1}{(\omega_n^2+\varepsilon_{k'}^2)^2}|\Delta^*(\boldsymbol{R},\boldsymbol{k}')^2|\Delta^*(\boldsymbol{R},\boldsymbol{k}). \qquad (5c)
\end{aligned}$$

It is seen that $\Delta^*(\boldsymbol{R},\boldsymbol{k})$ consists of both the $\boldsymbol{k}$-dependent and $\boldsymbol{k}$-independent components, which are denoted as $\Delta_d^*(\boldsymbol{R},\boldsymbol{k})$ and $\Delta_s^*(\boldsymbol{R})$, accordingly. To identify them, we make the following sanction:

$$V(\boldsymbol{k}-\boldsymbol{k}') = V_d(\hat{\boldsymbol{k}}_x^2 - \hat{\boldsymbol{k}}_y^2)(\boldsymbol{k}_x'^2 - \hat{\boldsymbol{k}}_y'^2) + V_s, \qquad (6)$$

$$\Delta^*(\boldsymbol{R},\boldsymbol{k}) \equiv \Delta_d^*(\boldsymbol{R})(\hat{\boldsymbol{k}}_x^2 - \hat{\boldsymbol{k}}_y^2) + \Delta_s^*(\boldsymbol{R}), \qquad (7)$$

where $\boldsymbol{k}$ is the unit vector in the direction of $\boldsymbol{k}$. Thus,

from Eqs.(5), $\Delta_{\rm s}^*(\boldsymbol{R})$ and $\Delta_{\rm d}^*(\boldsymbol{R})$ are given by

$$\begin{aligned}\Delta_{\rm s}^*(\boldsymbol{R}) =&N(0)V_{\rm s}\Delta_{\rm s}^*\ln\frac{2{\rm e}^{\gamma}\omega_{\rm D}}{\pi T}-\frac{7\zeta(3)}{8(\pi T)^2}N(0)V_{\rm s}\\ &\cdot\left\{\frac{1}{4}v_{\rm F}^2\Pi^2\Delta_{\rm s}^*+\frac{1}{8}v_{\rm F}^2(\Pi_x^2-\Pi_y^2)\Delta_{\rm d}^*\right.\\ &\left.+\Delta_{\rm s}\Delta_{\rm s}^{*2}+\frac{1}{2}\Delta_{\rm s}\Delta_{\rm d}^{*2}+|\Delta_{\rm d}|^2\Delta_{\rm s}^*\right\},\end{aligned}\tag{8}$$

$$\begin{aligned}\Delta_{\rm d}^*(\boldsymbol{R}) =&\frac{1}{2}N(0)V_{\rm d}\Delta_{\rm d}^*\ln\frac{2{\rm e}^{\gamma}\omega_{\rm D}}{\pi T}-\frac{7\zeta(3)}{8(\pi T)^2}N(0)V_{\rm d}\\ &\cdot\left\{\frac{1}{8}v_{\rm F}^2\Pi^2\Delta_{\rm d}^*+\frac{1}{8}v_{\rm F}^2(\Pi_x^2-\Pi_y^2)\Delta_{\rm s}^*\right.\\ &\left.+\frac{3}{8}\Delta_{\rm d}\Delta_{\rm d}^{*2}+\frac{1}{2}\Delta_{\rm d}\Delta_{\rm s}^{*2}+|\Delta_{\rm s}|^2\Delta_{\rm d}^*\right\},\end{aligned}\tag{9}$$

where $N(0)$ is the density of state at the Fermi surface, γ is the Euler constant, $v_{\rm F}$ is the Fermi velocity, and $\omega_{\rm D}$ is the average Debye frequency or the cut-off frequency for the interactions. (Note that Ting and co-workers have reported a G-L model for d-wave superconductors.[16] In their derivation, the s-wave component is thought of being an unpaired channel by assuming a positive repulsive interaction $V_{\rm s}$. As the authors recognized, their equation for $\Delta_{\rm s}$ would lead to some solutions without physical meaning, and the Pade approximation is used to avoid the singularity of the equation.) We should mention, however, that there is no *a priori* reason to assume pure d-wave symmetry for high-$T_{\rm c}$ superconductors; if such a state is present, it should follow from the Gor'kov model. We define $T_{\rm s}$ and $T_{\rm d}$ to be the apparent superconducting transition temperatures for the s- and d-wave channels, respectively.

$$N(0)V_{\rm s}\ln\frac{2{\rm e}^{\gamma}\omega_{\rm D}}{\pi T_{\rm s}}=1,\quad N(0)V_{\rm d}\ln\frac{2{\rm e}^{\gamma}\omega_{\rm D}}{\pi T_{\rm d}}=\frac{1}{2}.\tag{10}$$

The Ginzburg-Landau wavefunctions then follow from Eqs.(8) and (9):

$$\begin{aligned}&-\Delta_{\rm s}^*\ln\frac{T_{\rm s}}{T}+\frac{7\zeta(3)}{8(\pi T)^2}\left\{\frac{1}{4}v_{\rm F}^2\Pi^2\Delta_{\rm s}^*\right.\\ &+\frac{1}{8}v_{\rm F}^2(\Pi_x^2-\Pi_y^2)\Delta_{\rm d}^*+\Delta_{\rm s}\Delta_{\rm s}^{*2}\\ &\left.+\frac{1}{2}\Delta_{\rm s}\Delta_{\rm d}^{*2}+|\Delta_{\rm d}|^2\Delta_{\rm s}^*\right\}=0,\end{aligned}\tag{11}$$

$$\begin{aligned}&-\frac{1}{2}\Delta_{\rm d}^*\ln\frac{T_{\rm d}}{T}+\frac{7\zeta(3)}{8(\pi T)^2}\left\{\frac{1}{8}v_{\rm F}^2\Pi^2\Delta_{\rm d}^*\right.\\ &+\frac{1}{8}v_{\rm F}^2(\Pi_x^2-\Pi_y^2)\Delta_{\rm s}^*+\frac{3}{8}\Delta_{\rm d}\Delta_{\rm d}^{*2}\\ &\left.+\frac{1}{2}\Delta_{\rm d}\Delta_{\rm s}^{*2}+|\Delta_{\rm s}|^2\Delta_{\rm d}^*\right\}=0.\end{aligned}\tag{12}$$

Denoting $\alpha=7\zeta(3)/(8\pi T)^2$, we define $\Delta_0=\sqrt{4/3\alpha}$, and the coherence length at zero temperature to be $\xi_0=v_{\rm F}\sqrt{\alpha}/2$, and cast the above Ginzburg-Landau equations into dimensionless form by introducing $\boldsymbol{r}/\xi_0\to\boldsymbol{r}$, $\Delta/\Delta_0\to\Psi$,

$$\begin{aligned}&-\Psi_{\rm s}^*\ln\frac{T_{\rm s}}{T}+\left\{\Pi^2\Psi_{\rm s}^*+\frac{1}{2}(\Pi_x^2-\Pi_y^2)\Psi_{\rm d}^*\right.\\ &\left.+\frac{4}{3}\Psi_{\rm s}\Psi_{\rm s}^{*2}+\frac{2}{3}\Psi_{\rm s}\Psi_{\rm d}^{*2}+\frac{4}{3}|\Psi_{\rm d}|^2\Psi_{\rm s}^*\right\}=0,\end{aligned}\tag{13}$$

$$\begin{aligned}&-\Psi_{\rm d}^*\ln\frac{T_{\rm d}}{T}+\left\{\Pi^2\Psi_{\rm d}^*+(\Pi_x^2-\Pi_y^2)\Psi_{\rm s}^*\right.\\ &\left.+\Psi_{\rm d}\Psi_{\rm d}^{*2}+\frac{4}{3}\Psi_{\rm d}\Psi_{\rm s}^{*2}+\frac{8}{3}|\Psi_{\rm s}|^2\Psi_{\rm d}^*\right\}=0.\end{aligned}\tag{14}$$

The free energy deduced from the above expressions is then given as

$$\begin{aligned}f=&-\frac{1}{2}N(0)[2\ln(T_{\rm s}/T)|\Delta_{\rm s}|^2V_{\rm s}\\ &+\ln(T_{\rm d}/T)|\Delta_{\rm d}|^2V_{\rm d}]\\ &+\frac{1}{2}N(0)\frac{7\zeta(3)}{8(\pi T)^2}\left[V_{\rm s}|\Delta_{\rm s}|^4+\frac{3}{8}V_{\rm d}|\Delta_{\rm d}|^4\right.\\ &\left.+\frac{1}{2}(V_{\rm d}+V_{\rm s})|\Delta_{\rm s}|^2|\Delta_{\rm d}|^2+\frac{1}{2}(V_{\rm s}\Delta_{\rm s}^{*2}\Delta_{\rm d}^2+V_{\rm d}\Delta_{\rm s}^2\Delta_{\rm d}^{*2})\right]\\ &+\frac{1}{8}N(0)\frac{7\zeta(3)}{8(\pi T)^2}v_{\rm F}^2\left[2V_{\rm s}|\Pi\Delta_{\rm s}^*|^2+V_{\rm d}|\Pi\Delta_{\rm d}^*|^2\right.\\ &+(V_{\rm s}\Pi_x^*\Delta_{\rm s}\Pi_x\Delta_{\rm d}^*-V_{\rm s}\Pi_y^*\Delta_{\rm s}\Pi_y\Delta_{\rm d}^*+V_{\rm d}\Pi_x^*\Delta_{\rm d}\Pi_x\Delta_{\rm s}^*\\ &\left.-V_{\rm d}\Pi_y^*\Delta_{\rm d}\Pi_y\Delta_{\rm s}^*)\right]+\frac{1}{2\mu_0}(\nabla\times\boldsymbol{A})^2.\end{aligned}\tag{15}$$

Equivalently, the Ginzburg-Landau free energy $(f/(N(0)V_{\rm d}\Delta_0)\to f)$ expressed in terms of $\Psi_{\rm s}$ and $\Psi_{\rm d}$ is

$$\begin{aligned}f=&\alpha_{\rm s}|\Psi_{\rm s}|^2+\alpha_{\rm d}|\Psi_{\rm d}|+\frac{4}{3}|\Psi_{\rm d}|^4+\frac{1}{2}|\Psi_{\rm d}|^4\\ &+\frac{8}{3}|\Psi_{\rm s}|^2|\Psi_{\rm d}|^2+\frac{2}{3}(\Psi_{\rm s}^{*2}\Psi_{\rm d}^2+\Psi_{\rm d}^{*2}\Psi_{\rm s}^2)+2|\Pi\Psi_{\rm s}|^2\\ &+|\Pi\Psi_{\rm d}|^2+\Pi_x^*\Psi_{\rm s}\Pi_x\Psi_{\rm d}^*-\Pi_y^*\Psi_{\rm s}\Pi_y\Psi_{\rm d}^*\\ &+\Pi_x^*\Psi_{\rm d}\Pi_x\Psi_{\rm s}^*-\Pi_y^*\Psi_{\rm d}\Pi_y\Psi_{\rm s}^*+\kappa^2(\nabla\times\boldsymbol{A})^2,\end{aligned}\tag{16}$$

with $\alpha_{\rm s}=-2\ln(T_{\rm s}/T)V_{\rm s}/V_{\rm d}$, and $\alpha_{\rm d}=-\ln(T_{\rm d}/T)$, and κ being the G-L parameter. We should mention that, similar to the models from the phenomenological account,[17,18] our G-L model would lead to two transition temperatures. There is, however, no convincing experimental evidence for the occurrence of two transitions although some specific heat measurements seemed to indicate the splitting of phase transition in the high-$T_{\rm c}$ system under a magnetic field up to 15 T. This problem can, however, be avoided once the actual orthorhombic distortion has been taken into account,

as done by the author in a recent publication.[19] Since the s- and d-channels that belong to the A_1 and B_1 representations are almost degenerate in a tetragonal crystal point group, we will choose T_s and T_d defined by Eq.(10) to be very close to each other. The s and d states can coexist in two kinds of combination, that is, s+d or s+id. It can be shown that the s+d state is not stable for our G-L model. While, a transition from d to s+id is favoured energetically since it is a transformation from a state with gap nodes to a nodeless state, which is expected to lower the free energy of the system. Therefore, we will assume T_d to be slightly higher than T_s. Hence T_d is referred to as the zero-field critical temperature T_c, while T_s is taken as the offset temperature of the upper critical field curve $H_{C2}(T)$. A least-squares fit to the experimental data of Ref.[20] gives T_s=91.50±0.06 K and T_d=92.50 K .

Assuming the external field to be zero, i.e. implying that the derivative terms vanish, we study the thermodynamics of our G-L equations (11) and (12). For the s+id state, we obtain $|\Delta_d|^2 = (4/\alpha)\ln(T_d/T_s)$, $|\Delta_s|^2 = (1/\alpha)\ln(T_s^3/T_d^2T)$ when $T < T_d$ and $T < T_s$. The solution indicates that the s-wave channel could be attractive only if $T < T^* \equiv T_s^3/T_d^2$. Thus, one can expect that, if the temperature is very close to the normal to superconducting transition temperature, the $YBa_2Cu_3O_{7-\delta}$ superconductor will behave as a d-wave superconductor. The vortex lattice, if it exists, is thus triangular, as indicated in Abrikosov's theory.[21] At a sufficient low temperature, typically when $T < T^*$, the mixed s-d state will be in action. The coupling between s and d waves will then lead to a new structure of the lattice, an oblique vortex, for instance, as observed in the small angle neutron scattering on $YBa_2Cu_3O_7$ samples.[22]

Ⅲ. THE SINGLE VORTEX AND VORTEX LATTICE STRUCTURE

We restrict ourselves to the case of an untwined $YBa_2Cu_3O_7$ superconductor in a uniform applied field normal to the CuO_2 plane of $YBa_2Cu_3O_7$. The problem is thus two-dimensional; the order parameters vary only in the CuO_2 plane, and the vector potential has only two nonzero components which lie in the CuO_2 plane. We denote the two-dimensional Euclidean coordinates by x and y, and A_x and A_y for the x- and y-components of the vector potential. We are interested in the solutions of the G-L model that gives periodic measurable quantities in the plane.[1)]

The measurable quantities $|\Psi|^2$, the induced magnetic field $\nabla \times \boldsymbol{A}$, and the supercurrent $\nabla \times \nabla \times \boldsymbol{A}$ are periodic if Ψ and $\boldsymbol{A}$ satisfy

$$\Psi_{s,d}(\boldsymbol{x}+\boldsymbol{t}_k) = \Psi_{s,d}(\boldsymbol{x})\exp(ig_k(\boldsymbol{x})) \quad k=1,2, \tag{17}$$

$$A(\boldsymbol{x}+\boldsymbol{t}_k) = A(\boldsymbol{x}) + \nabla g_k(\boldsymbol{x}) \quad k=1,2, \tag{18}$$

for all $\boldsymbol{x}=(x,y) \in \boldsymbol{R}^2$, where

$$g_k(\boldsymbol{x}) = C_k - \frac{1}{2}\overline{B}[1+\theta)t_{ky}x - (1-\theta)t_{tx}y] \quad k=1,2. \tag{19}$$

Here θ, C_1 and C_2 are arbitrary constants.[23] The average magnetic induction strength $\overline{B}$ is related to the number of vortex m and unit cell area $|\boldsymbol{t}_1 \times \boldsymbol{t}_2|$ by

$$\overline{B} = 2\pi m/|\boldsymbol{t}_1 \times \boldsymbol{t}_2|. \tag{20}$$

We choose the constants $\theta=-1$, C_1=0 and C_2=0 to reduce the periodic conditions (18) and (19) to their simplest form. We should mention that there is no agreement in the literature on the choice of those constants. Here, the choice of these is motivated by the fact that the phase of $\Psi_{s,d}$ will thus be the same at all vortices of the lattice. We assume, without loss of generality, $\boldsymbol{t}_1 = (aL, bL)^T$, $\boldsymbol{t}_2 = (0, L)^T$ with $L > 0$, $a > 0$, and b is a real number; a is referred to as the aspect ratio and b the lattice angle in Abrikosov's theory.[21] In principle, one should keep $\boldsymbol{a}$ and $\boldsymbol{b}$ as free parameters in the model. A proper (a,b) value should lead to a minimum free energy. For example, to the vortex lattice with hexatic order and rotational symmetry in the plane, the only admissible values are $a=\sqrt{3}$ and b=1. However, since our model is fully periodic in the y-direction, we may identify the domain Ω of a unit cell generated by $\boldsymbol{t}_1$ and $\boldsymbol{t}_2$ to be the rectangular $[aL,0]\times[0,L]^T$ by setting b=0 and leaving a free. The reduced periodic conditions then reads

$$\begin{aligned} &\Psi_{s,d}(x+aL,y) = \Psi_{s,d}(x,y)e^{iy\Phi/2}, \\ &\Psi_{s,d}(x,y+L) = \Psi_{s,d}(x,y), \end{aligned} \tag{21}$$

$$\begin{aligned} &A_x(x+aL,y) = A_x(x,y), \\ &A_x(x,y+L) = A_x(x,y), \end{aligned} \tag{22}$$

$$\begin{aligned} &A_y(x+aL,y) = A_y(x,y) + \Phi/L, \\ &A_y(x,y+L) = A_y(x,y), \end{aligned} \tag{23}$$

where $\Phi = a\overline{B}L^2$ is the magnetic flux in the unit cell.

We show numerically the properties of solution of the discrete G-L free energy (Eq.(16)) subject to the periodic conditions, using the relaxation approach.

1) Given two arbitrary vectors $\vec{\boldsymbol{t}}_1$ and $\vec{\boldsymbol{t}}_2$ that span $\vec{\boldsymbol{R}}^2$, we say that a function f is periodic with respect to the lattice cell specified by $\vec{t}_1$ and $\vec{t}_2$ if $f(\vec{x}+\vec{t}_k) = f(\vec{x})$ for k=1,2 and for all $\vec{\boldsymbol{x}} = (x,y) \in \vec{\boldsymbol{R}}^2$.

We choose $\Psi_{\rm s}(\Psi_{\rm s}^*)$, $\Psi_{\rm d}(\Psi_{\rm d}^*)$, A_x, and A_y as independent variables. The relaxation iteration formula is

$$\Psi_{\rm s}^{(n+1)} = \Psi_{\rm s}^{(n)} - \varepsilon_1(\partial f/\partial \Psi_{\rm s}^*)|^{(n)},$$
$$\Psi_{\rm d}^{(n+1)} = \Psi_{\rm d}^{(n)} - \varepsilon_2(\partial f/\partial \Psi_{\rm d}^*)|^{(n)}, \qquad (24)$$
$$A_x^{(n+1)} = A_x^{(n)} - \varepsilon_3(\partial f/\partial A_x)|^{(n)},$$
$$A_y^{(n+1)} = A_y^{(n)} - \varepsilon_4(\partial f/\partial A_y)|^{(n)}, \qquad (25)$$

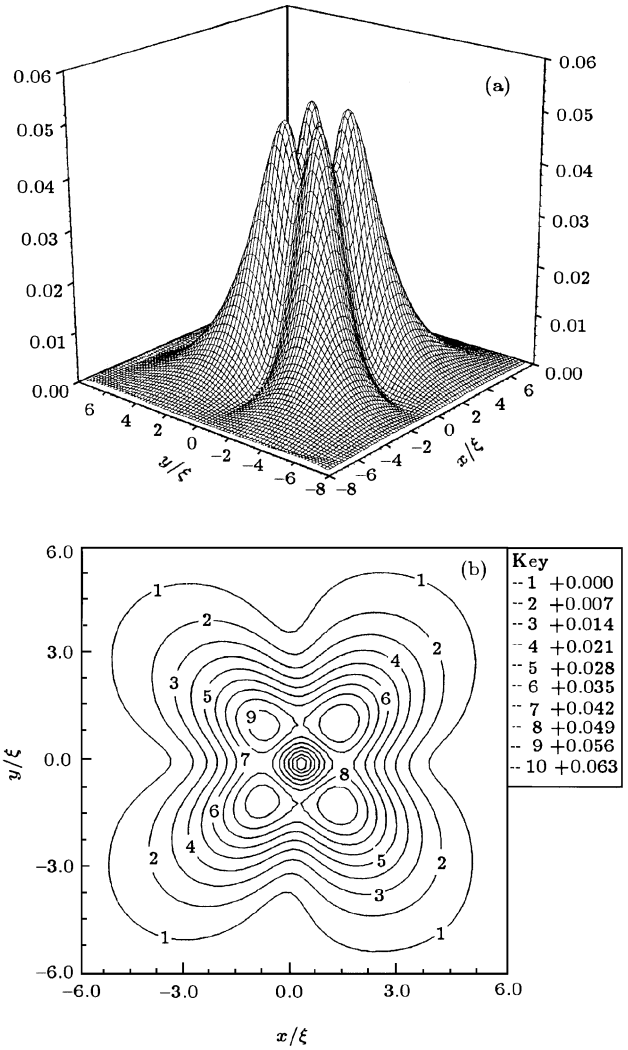


Fig.1. The surface (a) and contour (b) plots of s-wave component $|\Psi_{\rm s}|$ for $T/T_{\rm d}$=0.5, κ=5, and the vortices number per unit cell m=1.

where the relaxation factors ε's are positive numbers lying in (0, 2), and the integer n numbers the generation of iteration. It has been proven that f will monotonically converge to its global minimum value as n increases if the iteration emanates from a proper initial state.[24]

We set a=1 corresponding to a square unit cell and the vortices number m=1 to show the single vortex structure. We have assumed $T_{\rm d}$= 92.5K, $T_{\rm s}$=91.8K, and κ=5.[2)] We first choose T/T^*=0.5. The surface and contour plots of s-wave component are shown in figures 1(a) and 1(b). A fourfold symmetric distribution of $|\Psi_{\rm s}|$ is indicated, which leads to the anisotropy in $|\Psi_{\rm d}|$ (figure 2) and the local magnetic field h (figure 3) away from the vortex core. If we choose, on the other hand, temperature T beyond $T_{\rm s}$ but lower than $T_{\rm d}$, an explicit solution to the G-L equations (11) and (12) would be $|\Delta_{\rm d}|^2 = (4/3\alpha)\ln(T_{\rm d}/T)$, and $|\Delta_{\rm s}|^2 \to 0$. The numerical simulation reveals that $|\Psi_{\rm s}| \approx 10^{-3}$, and an isotropic distribution of $|\Psi_{\rm d}|$ and h recovers.

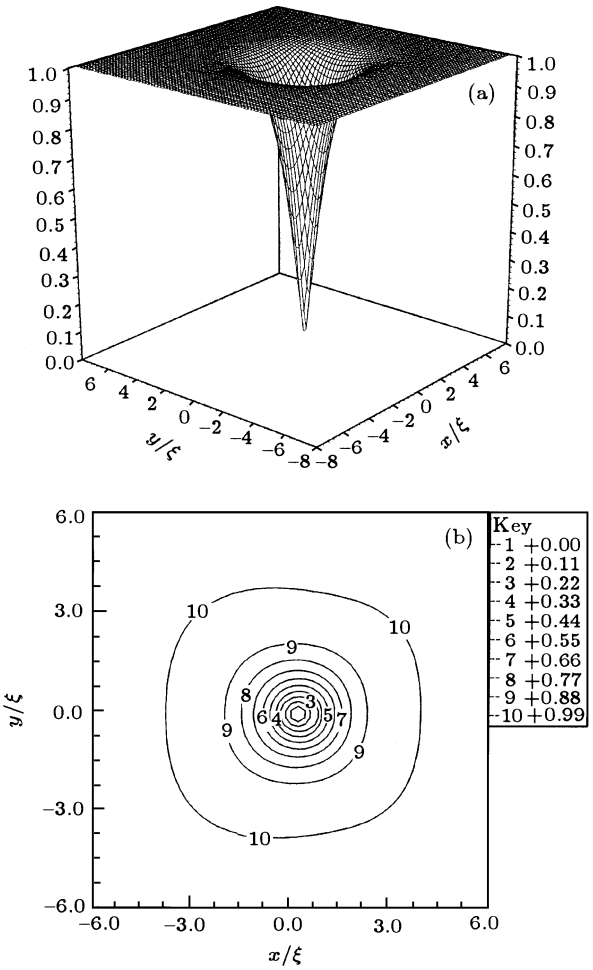


Fig.2. Spatial distribution of $|\Psi_{\rm d}|$ for $T/T_{\rm d}$=0.5, κ=5, and m=1: (a) surface plot and (b) contour plot.

[2)] By varying the G-L parameter κ, the feature of the single vortex remains unchanged qualitatively; however, the fourfold anisotropic contours of $\Psi_{\rm d}$ and h will move even far away from the vortex center as κ increases.

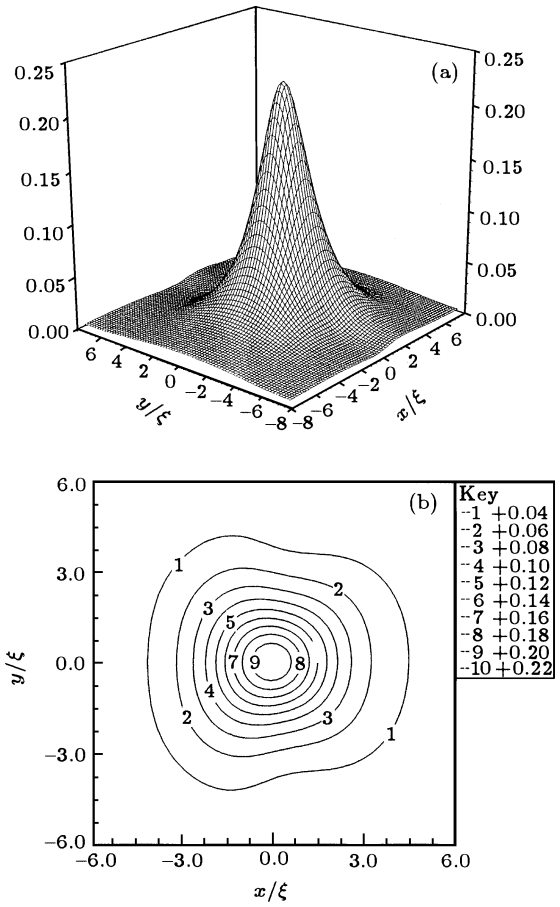


Fig.3. The local magnetic field h (figure 3): (a) surface plot and (b) contour plot. The same parameters are used as in figure 1.

We turn now to study the vortex lattice in a rectangular unit cell $[aL, 0] \times [0, L]^T$ with two vortices. It is known that the aspect ratio controls the shape of the vortex lattice. For example, a=1 signals a square lattice, while $a = \sqrt{3}$ gives a triangular lattice. We perform the minimization of the free-energy functional (16) with respect to a, while keeping the area of the unit cell constant. The unit cell is discretized into 64×64 meshes. The relaxation algorithm and periodic boundary condition described in preceding section are also used. Figure 4 gives a graph of the free energy associated with the minimum-energy configuration as a function of a, where we have chosen $T/T_{\rm d}$=0.5. The smallest value of the minimum free energy appears at $a_{\rm opt}$=1.3955, and an oblique vortex lattice of the local magnetic field is stable, as shown in figure 5. However, as T approaches $T_{\rm d}$, the minimum point of the free energy moves to $a_{\rm opt}$=1.75, and the triangular lattice is stable, as shown in figure 6. We should mention that the asymmetric configuration of the vortex lattice and a larger $a_{\rm opt}$ compared with the theoretical prediction are caused by the finite mesh size, and the symmetry is expected to recover in the limit as the mesh size goes to zero.

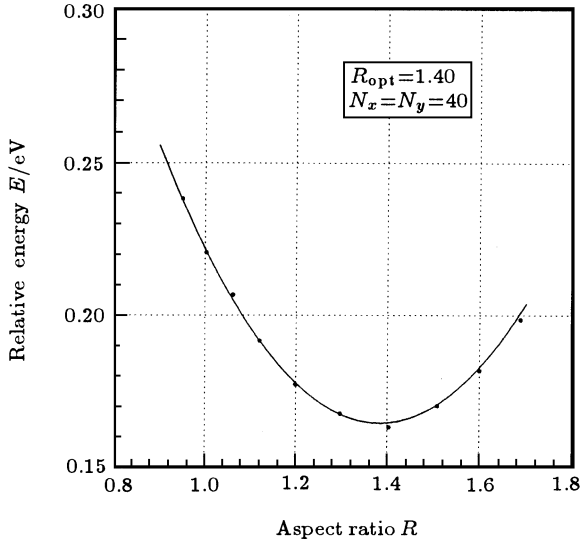


Fig.4. A graph of the minimum free energy configuration as a function of the aspect ratio a. We have chosen $T/T_{\rm d}$=0.5, κ=5, m=2, mesh numbers $N_x \times N_y$=40×40; and unit cell area aL^2=36$\sqrt{3}$. The smallest value of the minimum free energy appears at $a_{\rm opt}$=1.3955.

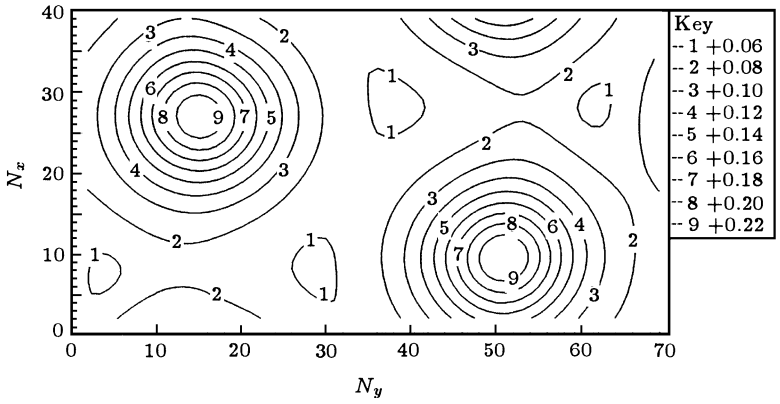


Fig.5. The contour plot of the local magnetic field h for $T/T_{\rm d}$=0.5, κ=5, m=2, N_x=40, N_y=64; and a=1.40, indicating an oblique vortex lattice.

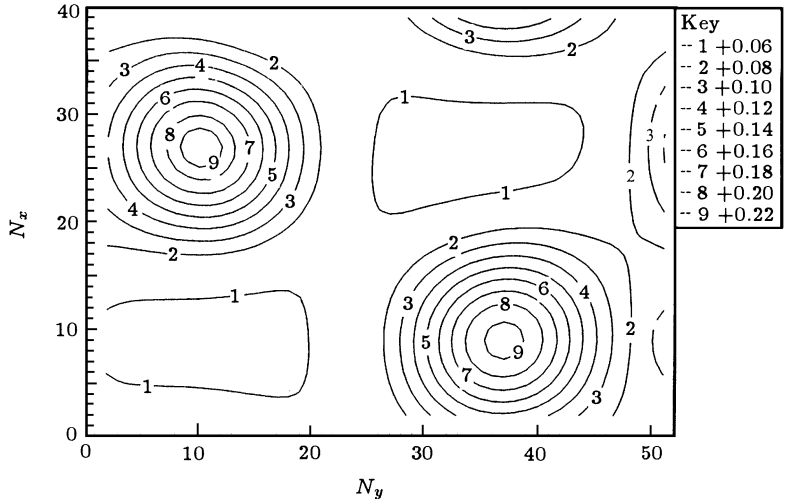


Fig.6. Same as figure 5 but $T/T_{\rm d}$=0.95 and a=1.75. A triangular lattice is then expected by replicating the solution in the unit cell.

IV. THE UPPER CRITICAL MAGNETIC FIELD $H_{\rm C2}(T)$

The detailed equilibrium behaviours of vortex phases in high-temperature superconductors, such as liquid, crystalline, glassy phases, and the K-T phase transition expected for a two-dimensional superconductor, promises to permanently alter the way we think about superconductivity. In particular, the unusual upward curvature of the upper critical field $H_{\rm C2}(T)$ near the critical temperature in the single-crystal $YBa_2Cu_3O_7$,[20] which is usually understood as a dimensional crossover of the diagram in layered superconductors,[25] can alternatively be interpreted as a possible evidence for unusual pairing symmetry.[17,26] We present computationally the upper critical field curve $H_{\rm C2}(T)$ to provide further support for this argument.

A perfect superconductor of type-II exposed to an applied magnetic field of increasing strength, the square of $|\Psi|$ decreases steadily until the sample enters the mixed state. The transition occurs at the lower critical field $H_{\rm C1}(T)$ where Ψ first vanishes and one or more vortices begin to form. Further increasing the field strength, a mixed to normal state transition occurs at the upper critical field $H_{\rm C2}$ where $\max\{|\Psi(x,y)| : (x,y) \in \Omega\} = 0$. Computationally, one can simulate this physical process by decreasing the size of the unit cell, while keeping the number of vortices per unit cell fixed. The procedure is based on the discrete virial theorem of Doria and co-workers[27]

$$\kappa^2 \overline{B} H = \frac{1}{2}(G_{\rm kin} + 2G_{\rm field}), \qquad (26)$$

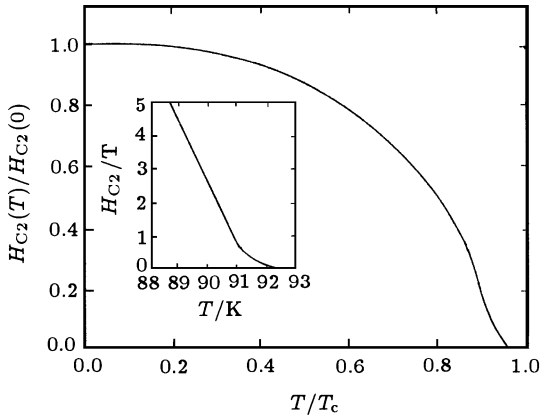


Fig.7. The plot of $H_{\rm C2}(T)$ as a function of temperature T for m=2, κ=5, and b=1, while a varying temperatures. The insertion is an enlarged drawing of $H_{\rm C2}(T)$ near the normal to superconducting transition temperature indicating an upward curvature of $H_{\rm C2}(T)$.

where the total free energy including the kinetic energy $G_{\rm kin}$ and field energy $G_{\rm field}$ per unit cell is given by $G_{\rm kin} = \int_\Omega f_{\rm kin} {\rm d}x{\rm d}y$, where f is defined by Eq.(11). In our practical settings, we decrease the unit cell length L, while keeping vortices number n fixed. Thus, we increase the average field induction $\overline{B}$. Having found the solution ($\Psi_{\rm s}$, $\Psi_{\rm d}$, A_x, A_y), we compute the total energy. The applied magnetic field H is then found from Eq.(26). The applied field where maximum $|\Psi_{\rm d,s}|^2$ vanishes corresponds to the upper critical field, accordingly. The plot of $H_{\rm C2}(T)$ as a function of temperature is given in figure 7. The data are for a two-vortex cell with κ=5, and b=1, with a varying temperatures. The insert is the enlarged drawing of $H_{\rm C2}(T)$ near the normal to superconducting transition temperatures indicating an upward curvature of $H_{\rm C2}(T)$, which can be interpreted as a result of the co-

existence of s and d waves in the sample. We present a plausible argument.

We define the creation and annihilation operators $p_+ = \sqrt{(\hbar c/2eH)/2}(\pi_x + \mathrm{i}\pi_y)$ and $p_- = \sqrt{(\hbar c/2eH)/2}(\pi_x - \mathrm{i}\pi_y)$. It follows from the G-L equations (13) and (14), to the leading order term, that

$$\begin{aligned}
&\alpha'_{\mathrm{s}} l^2 (T - T_{\mathrm{s}})\, \Psi_{\mathrm{s}}^* + \gamma_{\mathrm{s}} (2p_+ p_- + 1)\, \Psi_{\mathrm{s}}^* \\
&+ \gamma_v (p_+^2 + p_-^2)\, \Psi_{\mathrm{d}}^* = 0, \\
&\alpha'_{\mathrm{d}} l^2 (T - T_{\mathrm{d}})\, \Psi_{\mathrm{d}}^* + \gamma_{\mathrm{d}} (2p_+ p_- + 1)\, \Psi_{\mathrm{d}}^* \\
&+ \gamma_v (p_+^2 + p_-^2)\, \Psi_{\mathrm{s}}^* = 0,
\end{aligned} \tag{27}$$

where $l^2 = \hbar c/2eH$, $\alpha'_{\mathrm{s}} = \lambda_{\mathrm{s}}$, $\alpha'_{\mathrm{d}} = \lambda_{\mathrm{d}}$, $\gamma_{\mathrm{s}} = \alpha(T_{\mathrm{c}})\lambda_c v_f^2/4$, $\gamma_{\mathrm{d}} = \alpha(T_{\mathrm{c}})\lambda_{\mathrm{d}} v_f^2/4$ and $\gamma_v = \alpha(T_{\mathrm{c}})\lambda_{\mathrm{ds}} v_f^2/4$ with $\lambda_{\mathrm{s}} = (1/2)N(0)V_{\mathrm{s}}$, $\lambda_{\mathrm{d}} = (1/2)N(0)V_{\mathrm{d}}$, and $\lambda_{\mathrm{ds}} = (1/2)N(0)\sqrt{V_{\mathrm{d}}V_{\mathrm{s}}}$. Use of the commutation relation $[p_+, p_-] = 1$ has been made. Evidently, the left-hand side is a Hermitian operator acting on the state $(\Psi_{\mathrm{s}}, \Psi_{\mathrm{d}})$, whose eigenvalue is a function of H and T. The phase boundary $H_{\mathrm{C2}}(T)$ is the curve along which the lowest eigenvalue vanishes. We treat the problem in terms of perturbation theory. To the zeroth order in γ_v, Ψ_{s} and Ψ_{d} satisfy the uncoupled harmonic-oscillator equations, and the ground states are $|0\rangle_{\mathrm{s}}$ and $|0\rangle_{\mathrm{d}}$ satisfying $p_-|0\rangle_{\mathrm{s}} = 0$ and $p_-|0\rangle_{\mathrm{d}} = 0$ in an occupation number representation. In general, coupling between $|m\rangle_{\mathrm{s}}$ and $|n\rangle_{\mathrm{d}}$ is expected. To the first order in γ_v, however, $|0\rangle_{\mathrm{s}}$ couples only to $|2\rangle_{\mathrm{d}}$, and $|0\rangle_{\mathrm{d}}$ couples only to $|2\rangle_{\mathrm{s}}$. The lowest eigenvalues are given by

$$\begin{aligned}
&\frac{1}{2}[\alpha'_{\mathrm{s}} l^2 (T - T_{\mathrm{s}}) + \gamma_{\mathrm{s}} + \alpha'_{\mathrm{d}} l^2 (T - T_{\mathrm{d}}) + 5\gamma_{\mathrm{d}}] \\
&- \frac{1}{2}\{[\alpha'_{\mathrm{s}} l^2 (T - T_{\mathrm{s}}) + \gamma_{\mathrm{s}} \\
&- \alpha'_{\mathrm{d}} l^2 (T - T_{\mathrm{d}}) - 5\gamma_{\mathrm{d}}]^2 + 4\gamma_v^2\}^{1/2},
\end{aligned}$$

$$\begin{aligned}
&\frac{1}{2}[\alpha'_{\mathrm{d}} l^2 (T - T_{\mathrm{d}}) + \gamma_{\mathrm{d}} + \alpha'_{\mathrm{s}} l^2 (T - T_{\mathrm{s}}) + 5\gamma_{\mathrm{s}}] \\
&- \frac{1}{2}\{[\alpha'_{\mathrm{d}} l^2 (T - T_{\mathrm{d}}) + \gamma_{\mathrm{d}} \\
&- \alpha'_{\mathrm{s}} l^2 (T - T_{\mathrm{s}}) - 5\gamma_{\mathrm{s}}]^2 + 4\gamma_v^2\}^{1/2}.
\end{aligned}$$

The $H_{\mathrm{C2}}(T)$ equation obtained by setting the eigenvalue to zero is

$$[\alpha'_{\mathrm{d}} l^2 (T - T_{\mathrm{d}}) + \gamma_{\mathrm{d}}][\alpha'_{\mathrm{s}} l^2 (T - T_{\mathrm{s}}) + 5\gamma_{\mathrm{s}}]|_{H=H_{\mathrm{C2}}} = \gamma_v^2 \tag{28}$$

and a similar expression for s↔ d. As $T \to T_{\mathrm{c}}$, we find from this equation $H_{\mathrm{C2}} = (\alpha'_{\mathrm{d}}\hbar c/2e\gamma_{\mathrm{d}})(T_{\mathrm{d}} - T)$, reflecting the fact that there is no coupling between s and d waves as $H \to 0$ along the H_{C2} curve, as expected. For large H, on the other hand, $H_{\mathrm{C2}} = (a'_c\hbar c/10e\gamma_c)(T_{\mathrm{c}} - T)$ Thus, we find upward curvature in $H_{\mathrm{C2}}(T)$ since $V_{\mathrm{s}} >> V_{\mathrm{d}}$ (see Eq.(10), for instance).

V. CONCLUSION

We have derived microscopically, on the basis of Gor'kov approach, the Ginzburg-Landau equations for the superconductor with a cylindrical Fermi surface, and studied the vortex lattice structures of high-temperature superconductor $YBa_2Cu_3O_7$. The most remarkable feature of the vortex structure is the lattice transition from a triangle to an oblique as the temperature goes down from T_{d} to a lattice transition temperature T^*, below which the d and the s waves coexist. Coexistence of s and d waves is not surprising. Based on symmetry consideration, one could argue that the core of the vortex in the d-wave superconductor should involve all the possible order parameter functions that are consistent with the maximal symmetry group of the vortex line. In particular, it should have the conventional s-wave pairing with the opposite winding phase.[28,29]

We found that the internal degrees of freedom of the order parameters change along the $H_{\mathrm{C2}}(T)$ curve. For a superconductor with a mixed s-d state, the dominant $d_{x^2-y^2}$ wave at low fields turns to a superposition of s and d waves at high fields, accompanied by a distinct variation in the slope of $H_{\mathrm{C2}}(T)$. We should mention that the assumption of a pure d wave belonging to a two-dimensional representation will also lead to an upward curvature of $H_{\mathrm{C2}}(T)$. However, upward curvature for the two-dimensional d-wave case is produced only by the orthorhombic distortion that splits apart initially degenerate states, whereas the s and d order parameters are non-degenerate even in the absence of such a distortion. For the tetragonal high-T_{c} materials, we expect no upward curvature in H_{C2} for pure d-pairing symmetry. Thus, the existence of curvature for tetragonal Bi-Sr-Ca-Cu-O[30] signals evidently s–d pairing symmetry in this sample. We expect that further symmetric and extensive study of the vortex dynamics of high-T_{c} superconductors will shed light on the symmetry of the pairing state; a fundamental issue that bridges microscopic theory and experimental phenomenology of high-T_{c} superconductors.

References

[1] Monthoux P and Pines D 1994 *Phys. Rev.* B **49** 4261
[2] Monthonx P and Scalapino D J 1994 *Phys. Rev. Lett.* **72** 1874
[3] Zhang S C 1997 *Science* **275** 1089
[4] Wollman D A *et al* 1994 *Phys. Rev. Lett.* **71** 2134
[5] Tsuei C C *et al* 1994 *Phys. Rev. Lett.* **73** 593
[6] Chakravarty S, Sudbϕ A, Anderson P W and Strong S 1993 *Science* **261** 337
[7] Liechtenstein A I, Mazin I I and Andersen A I 1995 *Phys. Rev. Lett.* **74** 2303
[8] Millis A J 1994 *Phys. Rev.* B **49** 15408
[9] Kleiner R *et al* 1996 *Phys. Rev. Lett.* **76** 2161
[10] Kouzentsov K A *et al* 1997 *Phys. Rev. Lett.* **79** 3050
[11] Anderson P W 1987 *Science* **235** 1196
[12] Zhang F C and Rice T M 1988 *Phys. Rev.* B **37** 3759
[13] Lee P A and Read N 1987 *Phys. Rev. Lett.* **58** 2891
[14] Tinkham M 1964 *Group Theory and Quantum Mechanics* (New York: McGraw-Hill)
[15] Gor'kov L P 1960 *Sov. Phys. JETP* **9** 1364
[16] Yong Ren, Xu J H and Ting C S 1995 *Phys. Rev. Lett.* **74** 3680
[17] Joynt R 1990 *Phys. Rev.* B **41** 4271
[18] Li Q P *et al* 1993 *Phys. Rev.* B **48** 437
[19] Zhou S P 2000 *Physica* C **339** 258
[20] Welp U *et al* 1998 *Phys. Rev. Lett.* **62** 1908
[21] Abrikosov A 1957 *Zh. Eksp. Teor. Fiz.* **32** 1442
Abrikosov A 1957 *Sov. Phys. JETP* **5** 1174
[22] Keimer B *et al* 1994 *J. Appl. Phys.* **76** 6778
[23] Du Q, Gunzburger M D and Peterson J S 1993 *SIAM J. Appl. Math.* **53** 689
[24] Guo B Y 1988 *Numerical Methods for Partial Differential Equations* (Peking: Science Press) Chap 1 p43 (in Chinese)
[25] Ruggiero S, Barbie T and Beasley M 1982 *Phys. Rev.* B **26** 4897
[26] Zhou S P *et al* 1999 *Acta Phys. Sin.* **48** 342 (in Chinese)
[27] Doria M M, Gubernatis J E and Rainer D 1989 *Phys. Rev.* B **39** 9573
[28] Volovik G E 1993 *JETP Lett.* **58** 469
[29] Soininen P I, Kallin C and Berlinsky A J 1994 *Phys. Rev.* B **50** 13883
[30] Palstra T T *et al* 1988 *Phys. Rev. Lett.* **61** 1662